ARPN Journal of Engineering and Applied Sciences

www.arpnjournals.com

INCROP ZONE DEMARCATION OF COAL SEAM USING ELECTRICAL RESISTIVITY TOMOGRAPHY-A CASE STUDY OF A COAL BLOCK IN THE MAIN BASIN OF THE SINGRAULI COAL FIELD

Satyaveer Singh[1], Annapurna Barouah[1] and Vipin Kumar[2]
[1]University of Petroleum and Energy Studies, Dehradun, UK, India
[2]Central Mine Planning and Design Institute CIL RI, Singrauli Madhya Pradesh, India
E-Mail: satya.itbhu10@gmail.com

ABSTRACT

Delineation of Coal seam incrop zone is necessary for mine economics and coal conservation during mining operation. In this study demarcation of the incrop zone of a coal seam has been done by using the Electrical Resistivity Tomography method of Geophysical Electrical Resistivity survey. The resistivity data acquisition of the subsurface has been carried out by a 48-channel resistivity meter in the incrop zone of coal seams of the Main basin of the Singrauli coalfield. The resistivity of the subsurface in 2D sections along the 1000m survey lines is measured and plotted with the help of inversion techniques using RES2DINV software to depict the actual lithology of the subsurface in an Electrical resistivity imaging survey. The resistivity of the subsurface varies according to the geological characteristic of the rock, porosity, saturation of water, mineral and fluid content, etc. in the rock, and the resistivity of coal seams is generally higher than sedimentary country rock. The characteristics of higher resistivity of coal seam compared to country rock are helpful to demarcate the actual position of coal seam incrop zone. Resistivity variations of the subsurface are well correlated with geological formation as provided in available borehole lithology. Electrical Resistivity Tomography is effectively used to delineate the incrop zone of coal seams. The resistivity imaging survey is more economical and environmentally friendly in comparison to the conventional drilling method to prove the incrop zone of the coal seam.

Keywords: resistivity, imaging, inversion, tomography, incrop zone.

Manuscript Received 21 May 2024; Revised 1 December 2024; Published 10 January 2025

INTRODUCTION

Electrical Resistivity Tomography is an electrical resistivity imaging survey to evaluate the distribution of subsurface resistivity by sending electrical current in the subsurface and measuring its response on the surface by suspended electrodes into the surface. Electrical resistivity surveys are a very effective tool to carry out a subsurface investigation in hydrogeological, mining, geotechnical, environmental, and even hydrocarbon exploration (Loke *et al*., 2007) as well as to demarcate the hydrogeologic location and position of coal seam incrop zone (Das, 2015). The electrical resistivity method is used to measure variation in the electrical resistivity of the subsurface. The resistivity of any material is the resistance generated by a unit cube when a unit current passes normal to its surface. The resistivity of different formations has different resistivity due to variations in mineral, electrolyte, and water level saturation. The 2D resistivity survey method is very useful and most cost-effective in the investigation of elongated geological structures (Dahlin *et al*., 2002). Hydrogeological surveys become very easy and accurate with the implementation of Electrical resistivity imaging (Vu *et al*., 2021). Investigation and resolution generated in Electrical resistivity imaging are useful to decipher only the shallow sub-subsurface. The accuracy of the Electrical resistivity survey is limited to the shallow depth of the subsurface (Loke, 2015).

The resistivity measurement survey is based on the basic principle of resistance measurement during current flow between four-electrode devices (Zubair *et al.*, 2020). The measurement of resistivity is affected by the thickness of the layer and depth of occurrence in the subsurface. The resistivity of the subsurface has been measured with a combination of 4 Nos. of electrodes suspended into the surface. Two electrodes work as a transmitter (Current electrodes) and the other two as a receiver (Potential electrodes). Based on the separation of the electrodes several configurations of electrodes (Array) can be assigned during the measurement of subsurface resistivity.

The measured resistivity of the surface in a specific array is the apparent resistivity of the pseudo-section. Sensitivity is the degree to which a change in the resistivity of a pseudo section of the sub-surface will influence the potential measured in a specific array configuration. This apparent resistivity of the pseudo-section is converted into the actual resistivity of the subsurface with the help of Inversion techniques. The inversion technique in Electrical Resistivity Tomography is to accurately correlate the measured apparent resistivity value in a specific array configuration to the actual resistivity of the subsurface. The inversion modelling is done with the help of the Finite element or Finite difference method of numerical modelling techniques (Jaysaval *et al*., 2022). Linearized least-square with local optimization technique is generally used in 2D inversion for correlation of resistivity data (Sharma & Verma, 2015).

ARPN Journal of Engineering and Applied Sciences

An electrical resistivity survey can be very useful in the confirmation of structural features like faults which can be demarcated by a profound sudden change in the resistivity values within a resistivity layer (Hasan *et al.*, 2021). The resistivity layer will appear to shift or terminate when a fault is encountered across the survey lines. Nonetheless, since the depth of investigation of this survey is less, in most cases the downthrown side of the fault is not covered and not visible in the section making interpretation difficult. The throw of the fault cannot be deciphered in this case. However, the result produced by this survey is a good supplement to other exploratory data (Day-Lewis *et al.,* 2005).

The structure of coal seams incrop zones has a lot of uncertainty and undulations. To prove the accurate structure of coal seams incrop zones requires a lot of drilling of boreholes, which is time-consuming and cost-intensive work. Electrical Resistivity Tomography can be used to decipher the structure and extent of coal seams in an incrop zone area. As the coal has moderately high resistivity than sandstone and shale, so a change in resistivity will appear due to the occurrence of coal in the sub-surface during the electrical resistivity imaging survey.

Array Configuration

The electrical resistivity method is based on the fundamental theory of direct-current (DC) resistivity exploration (Zhou, 2018). The basic setup of 4 Nos. of electrodes for resistivity measurement is shown in Figure-1.

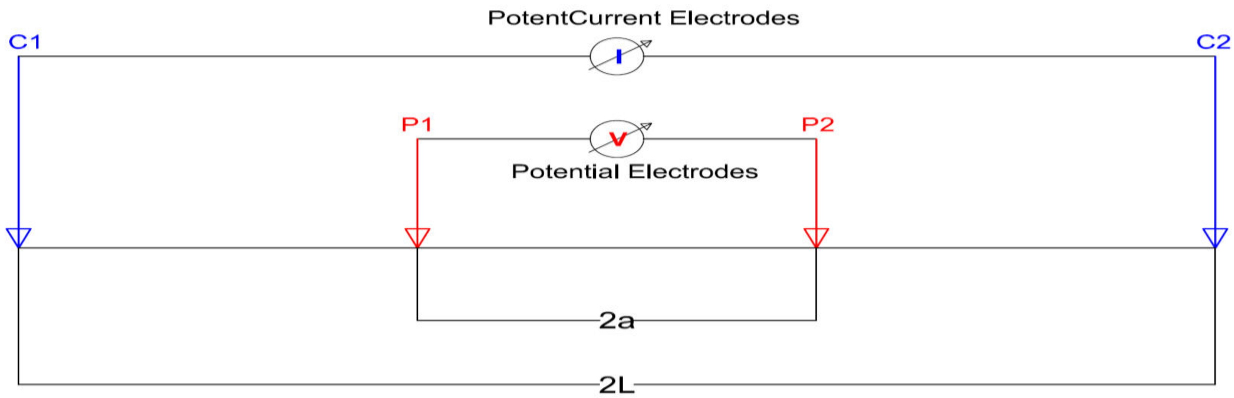

Figure-1. Representative setup for Resistivity measurement.

The basic electricity equation for the configuration is given below:

$$\rho a = K (V/I) \quad (1)$$

where, ρ_a= Apparent Resistivity of the medium

V = Potential (volts)
I = Current (ampere)
K = Geometrical factor

$$\text{Geometrical Factor } (K) = \pi \times (L^2-a^2) / 2a \quad (2)$$

where, L=Half of the separation distance between current electrodes in meter

a= Half of the separation distance between potential electrodes in meter

Array configuration is a sequence of electrode configurations in which measured electrical resistivity data are acquired. Based on electrode configuration and its separation, several array configurations of electrodes can be created. There are mainly five types of array arrangement used in Electrical resistivity imaging surveys: i) Wenner, ii) Dipole-dipole iii) Wenner - Schlumberger, iv) Pole-pole and v) Pole-dipole

All array configurations have some advantage over others, Wenner - Schlumberger has both reasonably good horizontal and vertical resolution. To get a better result combination of array configuration may be used. The combination of Wenner - Schlumberger and Dipole-dipole array arrangement provides the benefit of strong signal-to-noise ratio and vertical sensitivity of Wenner - Schlumberger as well as sensitivity to lateral changes of Dipole-dipole both to provide maximum subsurface information with higher accuracy (Hamdan & Vafidis, 2009).

STUDY AREA

The coal block is situated in the Main Basin of the Singrauli coalfield (Latitude- 23°46'37" N to 24°13'17" N and Longitude- 81°45'24" E to 82°47'50" E) in the Singrauli district of Madhya Pradesh, India. The geological formation of this Coal field consists of Barren Measures and the Barakar Formation of the Lower Gondwana Group and somewhere Raniganj Formation also occurs. Most of the area is covered by the sediments of Barakar and the sediments of Barren-Measure formation with a thin cover of soil and alluvium. Eight

VOL. 19, NO. 23, DECEMBER 2024 ISSN 1819-6608
ARPN Journal of Engineering and Applied Sciences

coal seams of the Barakar formation occur in the coal block. This coal block is situated on a plateau type of formation and coal seams are dipping westerly having strike direction N-S. The study has been conducted to depict the incrop zone of the upper two potential coal seams, namely seam-VIII and seam-VII. The thickness of uppermost coal seam-VIII varies between 2-3m, and of seam-VII varies between 12-15m. Sandstone, shaly sandstone, and alluvium soil are mainly found incrop zones of coal seams. Five number of boreholes are available in this area, which has been used to correlate the study. Five survey lines, approximately perpendicular to the expected incrop of coal seams of 1000m in length and 200m apart from each other have been demarcated for electrical resistivity survey. These five survey lines have been marked on the topography plan with available drilled boreholes, which are shown in Figure-2.

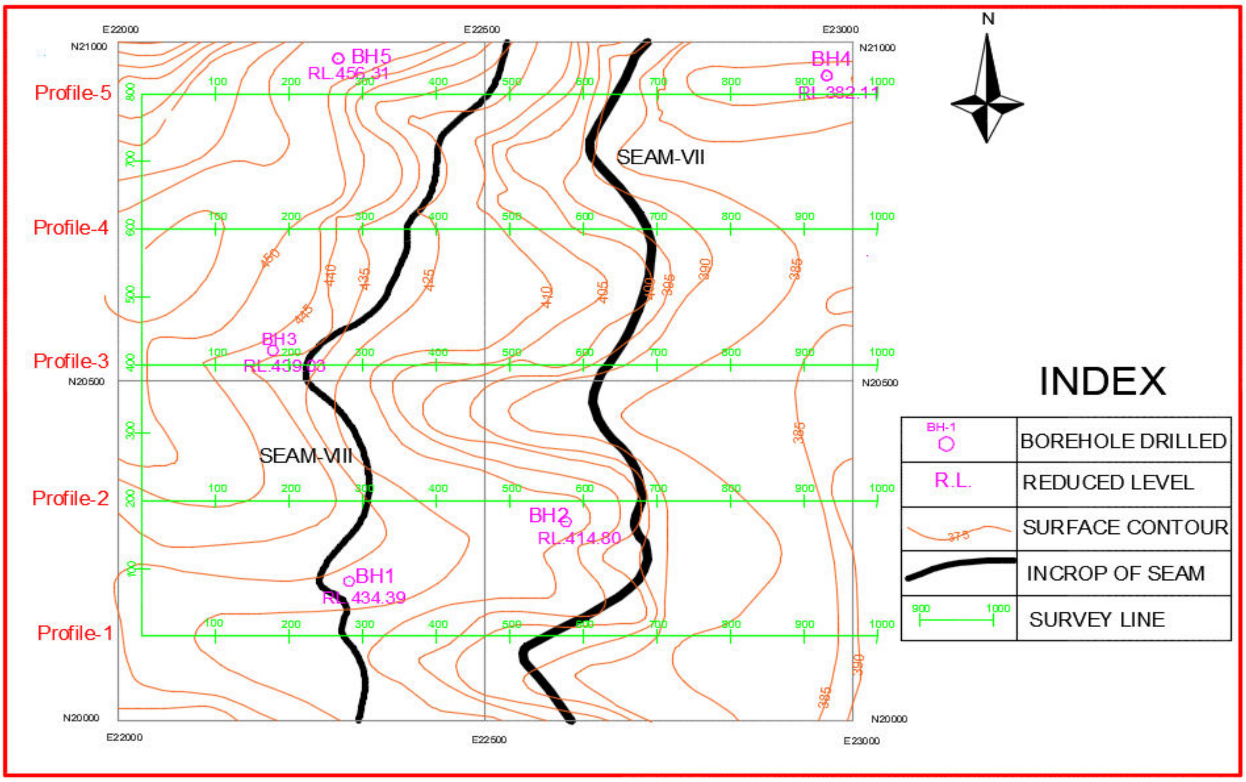

Figure-2. Survey lines marked on surface topography plan.

The electrode sequences (array) are designed in the Electre-Pro software. The data acquisition has been carried out by the IRIS make 48 channel resistivity meter with Wenner-Schlumberger array electrode configurations. In this configuration, both the Wenner profiling and the Schlumberger sounding are measured in a single run. Each data corresponding to an electrode configuration is measured and stored temporarily in the built-in memory of the instrument according to the sequence chosen for data acquisition. This setup has been moved forward to carry out further resistivity data acquisition for all survey lines.
The entire survey has been divided into three stages i.e. data acquisition, data processing, and data inversion and interpretation. After data acquisition is completed, the noise and outliers from the data are removed during the processing of the data by Prosys-II software. The depth of investigation in data processing by the software was fixed to 50m to avoid the influence of lower coal seams, which exist beneath the coal seam-VII. Inversion of the processed data is done by the RES2DINV software. An inverted section with resistivity distribution is plotted between the depth and the distance from the first electrode by the software as an output. The inverted section along all the profile lines is well correlated with the available geological data of drilled boreholes.

RESULT AND DISCUSSIONS

The resistivity shown in the resistivity section is represented in ohm-metre. The total dissolved solid is an electrolyte for electrical conductance, so a high TDS in saturated water levels shows less resistivity (Little *et al*., 2018). The top surface layer of the area consists of alluvium soil and has a slightly high resistivity value due to low water content, but the layer beneath this generally consists of water-saturated sandstone showing low resistivity (Taiwo, 2017). If a coal seam occurs in this area resistivity will change significantly which can be distinguished from nearby formations (Huang *et al*.,

VOL. 19, NO. 23, DECEMBER 2024 ISSN 1819-6608
ARPN Journal of Engineering and Applied Sciences

2020). The coal-bearing area shows a high resistivity value ranging from 600-1000 ohm-metre (Krishnamurthy *et al.*, 2009). The low resistivity area is demarcated by alluvium soil, and sandstone with a saturated water level, while the high resistivity area is demarcated by coal-bearing area. Saad has studied the resistivity of common rocks and soil material, which are tabulated in Table-1 (Saad *et al.*, 2012).

Table-1. Resistivity value of common rocks and soil material.

Material	**Resistivity** (ohm-metre)
Alluvium	10 - 800
Sand	60 to 800
Clay	1 to 100
Groundwater (fresh)	10 to 100
Sandstone	$8\text{-}4\times10^3$
Shale	$20\text{-}2\times10^3$
Limestone	$50\text{-}4\times10^3$
Granite	5000 to 1000000

The measured resistivity data has been processed for inversion with RES2DINV software. Electrical Resistivity Tomograms (ERT) in the form of an inverted section of each profile line are plotted as a colour map with a log resistivity scale and x-axis represents the distance from the first electrode and the y-axis represents elevation as reduced level (RL in m) of the profile line. The inverted section of each profile line has been discussed to depict the subsurface lithology and structural features. As per the lithology of available boreholes in the area, Coal seam-VIII is the topmost coal seam and its thickness is around 2m (thin seam), so the effect of coal seam in terms of resistivity (sensitivity function) measurement will be less. Coal seam-VII occurs beneath the coal seam-VIII and its thickness is around 14m (thick seam), so the effect of coal seam in terms of resistivity (sensitivity function) measurement will be greater. The depiction of coal seams will be done accordingly. Five number of boreholes are available in this area, which are drilled for reserve estimation. The five available boreholes are not sufficient to prove an incrop zone of 1 km2. Borehole Lithologs of these boreholes are given in Figure-3. These borehole Lithologs have been used to correlate with the depiction done by the Electrical Resistivity Imaging Survey.

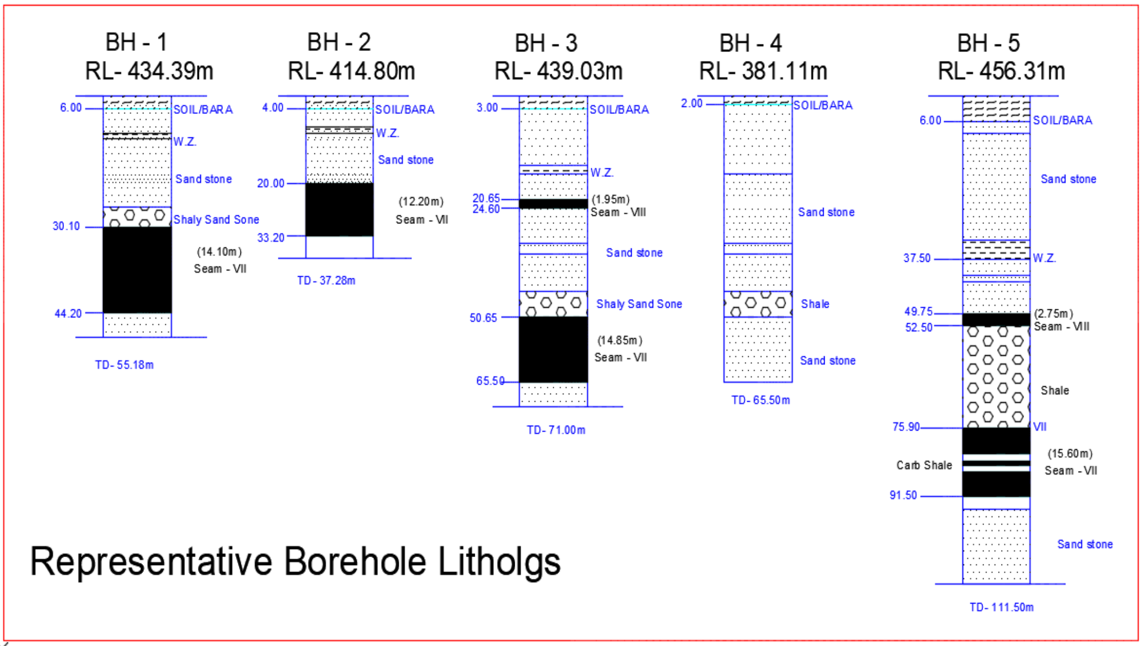

Figure-3. Representative Borehole Lithologs.

Profile-1

The position of Profile-1 is shown in Figure-2. The nearest borehole to Profile-1 is BH-1, which is about 300m apart from the origin point of Profile-1. The ERT result of the electrical resistivity imaging survey of Profile-1 has been shown in the form of an inverted resistivity section in Figure-4. The mean square error in ERT is 0.94. The resistivity in ERT ranges from 90 ohm-metre to 940 ohm-metre. The relatively high resistivity layer is demarcated by the coal-bearing area. Based on resistivity analysis, the occurrence of Coal seam-VIII is around up to 275m, and the occurrence of Coal seam-VII is around up to 550m from the origin of the profile-1. The depth of occurrence of coal seam-VII shown in borehole BH-1 is 30.10m and the nearly same depth of occurrence

VOL. 19, NO. 23, DECEMBER 2024 ISSN 1819-6608
ARPN Journal of Engineering and Applied Sciences

www.arpnjournals.com

of coal seam-VII is depicted in the ERT section shown in Figure-4.

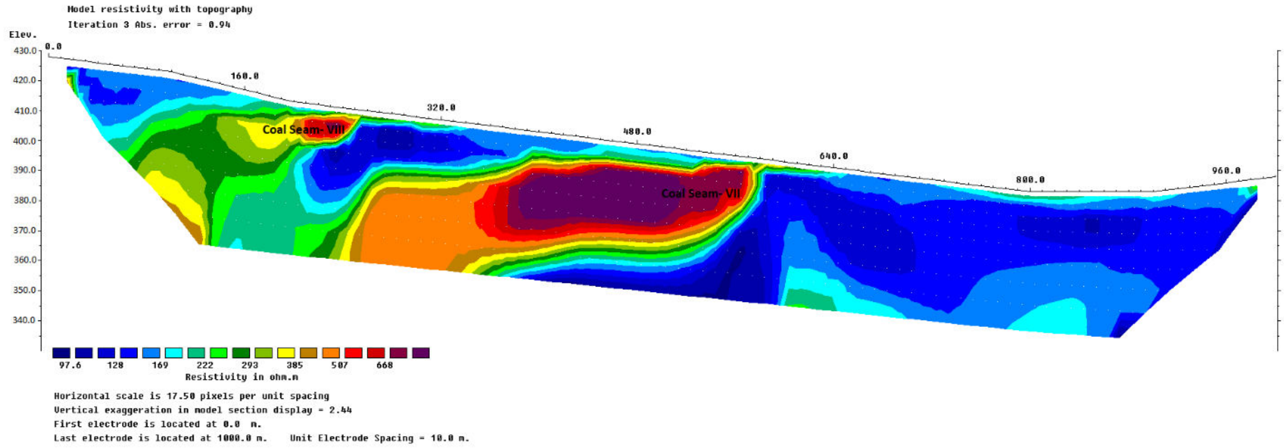

Figure-4. ERT of inverted resistivity section along Profile-1.

Profile-2

The position of Profile 2 is shown in Figure-2. The nearest borehole to Profile-2 is BH-2, which is about 550m apart from the origin point of Profile 2. The ERT result of the electrical resistivity imaging survey of Profile-2 has been shown in the form of an inverted resistivity section in Figure-5. The mean square error in ERT is 1.10. The resistivity in ERT ranges from 30 ohm-metre to 700 ohm-metre. The relatively high resistivity layer is demarcated by the coal-bearing area. Based on resistivity analysis, the occurrence of Coal seam-VIII is around up to 310m and the occurrence of Coal seam-VII is around up to 650m from the origin of the profile-2. The depth of occurrence of coal seam-VII shown in borehole BH-2 is 20.00m and the nearly same depth of occurrence of coal seam-VII is depicted in the ERT section shown in Figure-5.

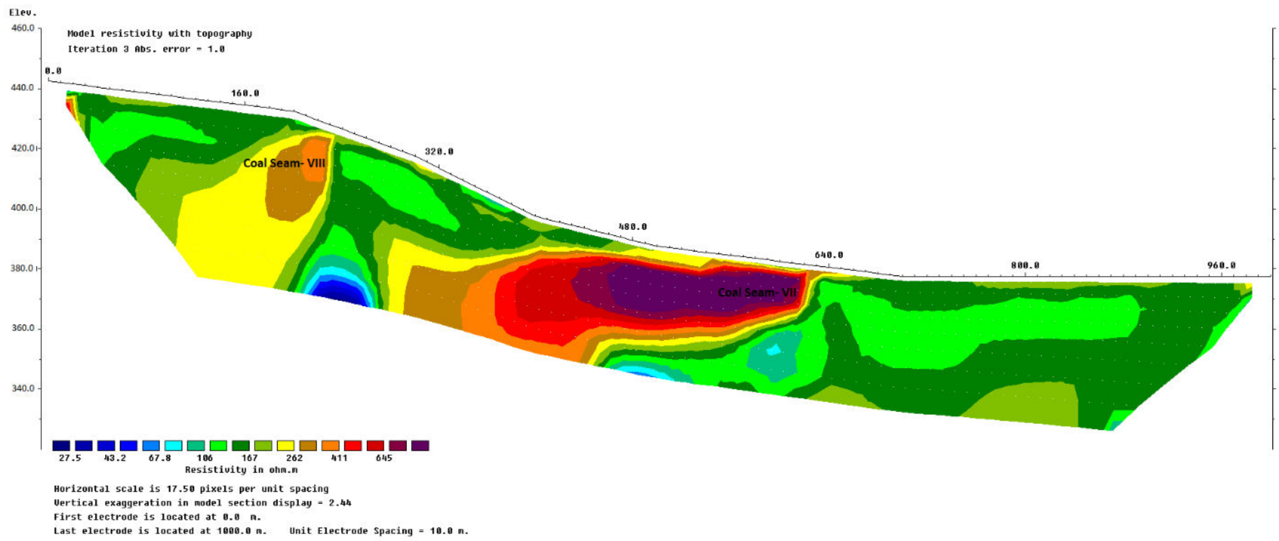

Figure-5. ERT of inverted resistivity section along Profile-2.

Profile-3

The position of Profile 3 is shown in Figure-2. The nearest borehole to Profile-3 is BH-3, which is about 200m apart from the origin point of Profile-3. The ERT result of the electrical resistivity imaging survey of Profile-3 has been shown in the form of an inverted resistivity -section in Figure-6. The mean square error in ERT is 1.0. The resistivity in ERT ranges from 25 ohm-metre to 1130 ohm-metre. The relatively high resistivity layer is demarcated by the coal-bearing area. Based on resistivity analysis, the occurrence of Coal seam-VIII is around up to 310m, and the occurrence of Coal seam-VII is around up to 650m from the origin of the profile-3. The depth of occurrence of coal seam-VIII and coal seam-VII shown in borehole BH-3 are 20.65m and 50.65m respectively. The depth of occurrence of coal seam-VIII and Coal seam-VII are nearly the same as depicted in the ERT section shown in Figure-6.

VOL. 19, NO. 23, DECEMBER 2024 ISSN 1819-6608
ARPN Journal of Engineering and Applied Sciences

www.arpnjournals.com

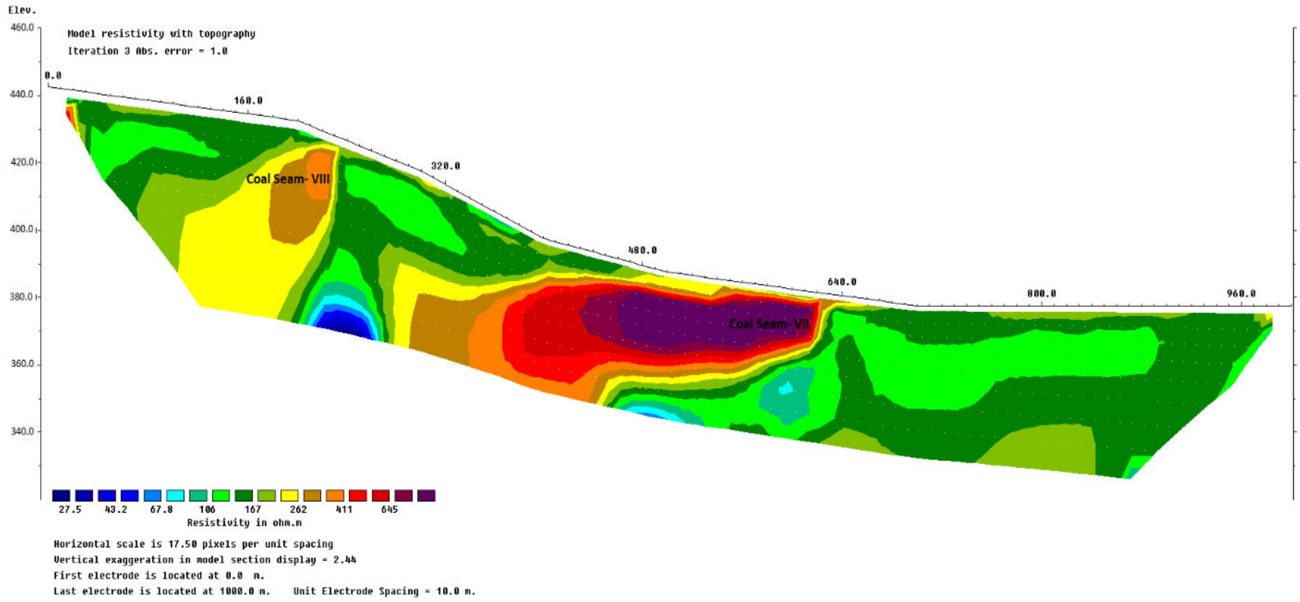

Figure-6. ERT of inverted resistivity section along Profile-3.

Profile-4

The position of Profile-4 is shown in Figure-2. No borehole is nearby to the Profile-4. The ERT result of the electrical resistivity imaging survey of Profile-4 has been shown in the form of an inverted resistivity -section in Figure-7. The mean square error in ERT is 1.10. The resistivity in ERT ranges from 80 ohm-metre to 810 ohm-metre. The relatively high resistivity layer is demarcated by the coal-bearing area. Based on resistivity analysis, the occurrence of Coal seam- VIII is around up to 360m, and the occurrence of Coal seam- VII is around up to 680m from the origin of the profile-4.

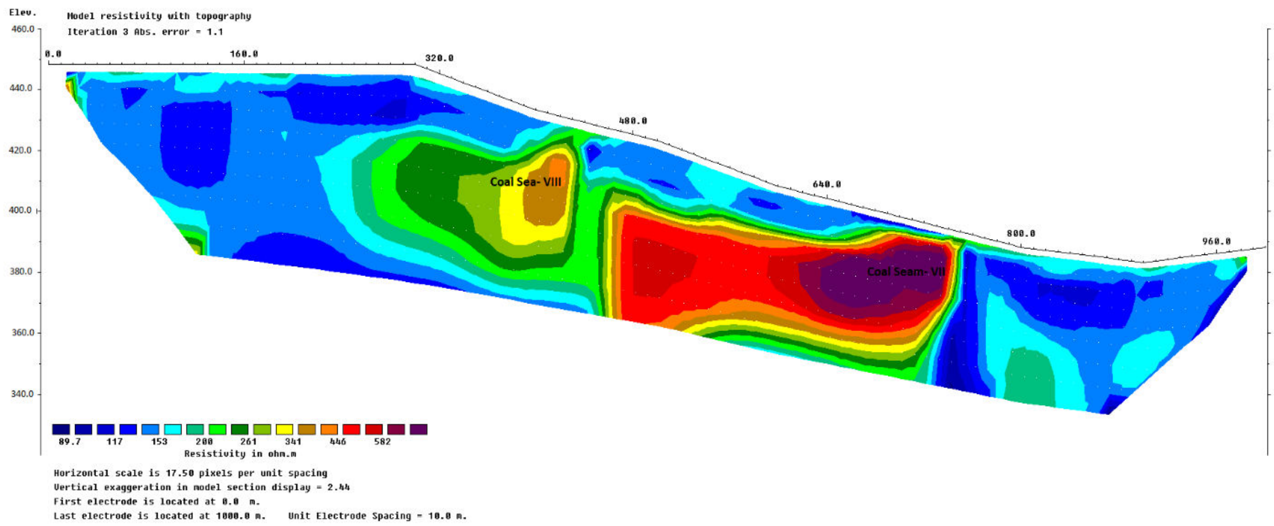

Figure-7. ERT of inverted resistivity section along Profile-4.

Profile-5

The position of Profile-5 is shown in Figure-2. The nearest boreholes to Profile-5 are BH-4 and BH-5, which are about 900m and 300m apart respectively from the origin point of Profile-5. The ERT result of the electrical resistivity imaging survey of Profile-5 has been shown in the form of an inverted resistivity section in Figure-8. The mean square error in ERT is 1.60. The resistivity in ERT ranges from 20 ohm-metre to 650 ohm-metre. The relatively high resistivity layer is demarcated by the coal-bearing area. Based on resistivity analysis, the occurrence of Coal seam- VIII is around up to 470m, and the occurrence of Coal seam- VII is around up to 645m from the origin of the profile-5. The depth of occurrence

VOL. 19, NO. 23, DECEMBER 2024 ISSN 1819-6608
ARPN Journal of Engineering and Applied Sciences

www.arpnjournals.com

of coal seam- -VIII and coal seam-VII shown in borehole BH-5 are 49.75m and 75.90m respectively. The depth of occurrence of coal seam-VIII and Coal seam- VII are not depicted in the ERT section shown in Figure-8, nearby to borehole BH-5 as the depth of investigation is restricted to 50m in ERT. No coal seam is encountered in borehole BH-4 and the same has been depicted in ERT of the inverted section shown in Figure-8 nearby to borehole BH-4.

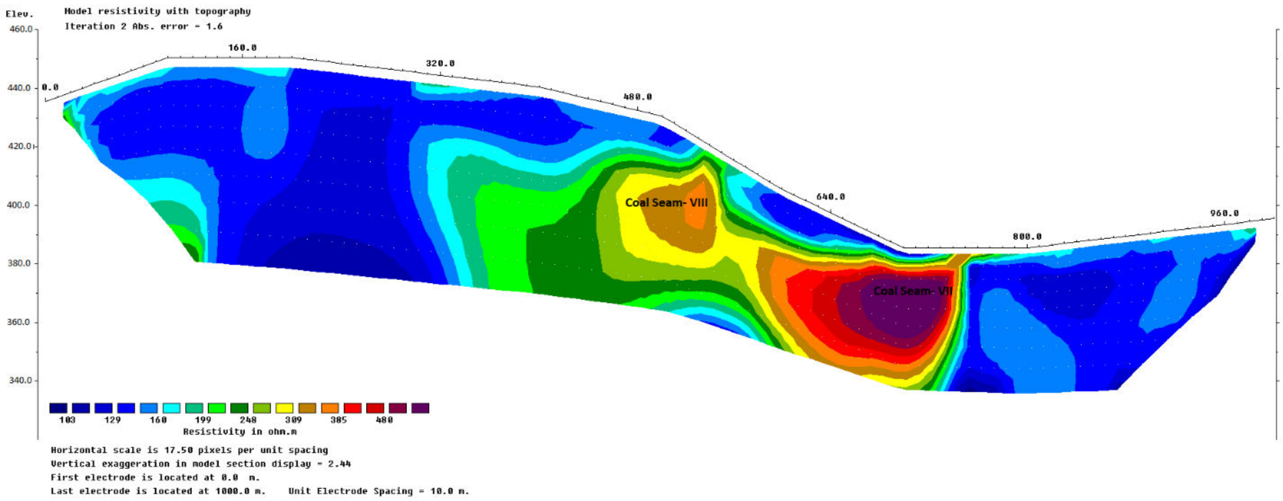

Figure-8. ERT of inverted resistivity section along Profile-5.

Profiles such as Profile-1, Profile-2, Profile-3, Profile-4, and Profile-5 have been meticulously examined, with attention to the proximity of boreholes (BH-1 to BH-5) and their correlation with ERT findings. The depth of occurrence of coal seams as indicated by boreholes aligns closely with the ERT-derived results, validating the effectiveness of the applied methodology. It is noteworthy that the mean square error in ERT ranges from 0.94 to 1.60, signifying a reasonable degree of accuracy in the resistivity analyses. The ERT sections visually represent the subsurface structures, allowing for the identification of coal seams and their extent within the study area.

The extent of coal seams Seam-VIII and Seam-VII incrop zone have been depicted by ERT of inverted resistivity section of the subsurface along the different Profiles of Electrical resistivity survey lines and the same has been marked on the topography plan shown in Figure-2. The depiction of coal seams by ERT is very well correlated with available borehole data and its lithology.

In this study, a comprehensive analysis of multiple profiles (Profile-1 to Profile-5) using Electrical Resistivity Tomography (ERT) has provided valuable insights into the subsurface coal-bearing formations. The study aimed to correlate the ERT results with existing borehole data and lithology, shedding light on the depth and occurrence of Coal Seam-VIII and Coal Seam-VII. The ERT results presented in inverted resistivity sections for each profile reveal distinct patterns of resistivity ranging from 20 ohm-metre to 1130 ohm-metre. The relatively high resistivity layers are indicative of coal-bearing areas, and their demarcation aligns with the occurrence of specific coal seams.

CONCLUSIONS

The study depicts the geological structure along with the material properties of the subsurface horizon layer. The profile (profile 1) is located near BH-1; ERT analysis indicated the presence of Coal Seam-VIII up to 275m and Coal Seam-VII up to 550m from the origin. Depth correlated with borehole BH-1 findings. The profile-2 positioned near BH-2, ERT results showcased Coal Seam-VIII up to 310m and Coal Seam-VII up to 650m from the origin, aligning with BH-2 data. Profile-3 positioned near BH-3, ERT outlined the occurrence of Coal Seam-VIII and Coal Seam-VII around 310m and 650m, respectively. Depths matched BH-3 findings. ERT analysis in Profile-4, lacking nearby boreholes, indicated Coal Seam-VIII up to 360m and Coal Seam-VII up to 680m from the origin. Adjacent to BH-4 and BH-5, ERT findings of profile -5 displayed Coal Seam-VIII around 470m and Coal Seam-VII around 645m from the origin. Depth correlation with BH-5, limited by the ERT depth of investigation, was achieved. ERT proved effective in delineating coal seams, providing a valuable non-intrusive method for subsurface exploration. Findings from ERT align closely with borehole data, validating the accuracy of the method. The study establishes a correlation between resistivity patterns and coal-bearing areas, offering a robust tool for future coal exploration projects. The successful application of ERT in mapping coal seams underscores its potential as a reliable and efficient technique in the field of geophysical exploration. The integration of ERT data with borehole information enhances the accuracy of subsurface characterization, providing valuable insights for geological and mining assessments.

The ERT technique is also found effective in demarcating standing coal pillars and de-coaled areas in old coal mine working, as the de-coaled area is filled with water having less resistivity while standing coal pillars have comparatively high resistivity and a contrast inverted section is achieved near the standing coal pillar indicating high resistive zone ranging from 600-1000 Ohm-metre (Krishnamurthy et al., 2009). The electrical resistivity imaging survey may also be done to prove the existence, fault, depth, and as well as thickness of coal seams with higher accuracy without going into costly and tedious drilling activities.

The conventional drilling method to prove crop zones is capital-intensive and time-consuming. The local perched water table may fluctuate due to the puncture of impervious rock during the drilling of boreholes and drilled boreholes may create an avenue for the unwanted environmental emission of greenhouse gas (methane) stored in coal seam. Pollution will be added due to the burning of diesel as an energy source for drilling activities and the splashing of lubricant. The resistivity imaging survey is a non-invasive method to investigate the subsurface. The resistivity imaging survey is more economical and environmentally friendly in comparison to the conventional drilling method to prove the incrop zone of the coal seam.

The findings from this study have practical implications for coal exploration and resource assessment. A resistivity imaging survey is a more effective tool than other conventional electrical survey as it acquires continuous electrical data with different configurations. The correlation between ERT data and borehole information enhances our understanding of the coal-bearing formations, providing crucial insights for future mining and resource management endeavors.

REFERENCES

Dahlin T., Bernstone C. and Loke M. H. 2002. A 3-D resistivity investigation of a contaminated site at Lernacken, Sweden. Geophysics, 67(6): 1692-1700. https://doi.org/10.1190/1.1527070

Das A. 2015. Identification of coal seam incrop position and groundwater aquifer zone by Electrical Resistivity Survey technique : A case study from Mahan Coal Block, (Issue June). https://doi.org/10.13140/RG.2.1.1399.0564

Day-Lewis F. D., Singha K. and Binley A. M. 2005. Applying petrophysical models to radar travel time and electrical resistivity tomograms: Resolution-dependent limitations. Journal of Geophysical Research: Solid Earth, 110(8): 1-17. https://doi.org/10.1029/2004JB003569

Hamdan H. and Vafidis A. 2009. Inversion techniques to improve the resistivity images over karstic structures. Near Surface 2009 - 15th European Meeting of Environmental and Engineering Geophysics, February. https://doi.org/10.3997/2214-4609.20147076

Hasan M., Shang Y., Meng H., Shao P. and Yi X. 2021. Application of electrical resistivity tomography (ERT) for rock mass quality evaluation. Scientific Reports, 11(1): 1-19. https://doi.org/10.1038/s41598-021-03217-8

Huang J., Liu S., Tang S., Shi S. and Wang C. 2020. Study on the coalbed methane development under high in situ stress, large buried depth, and low permeability reservoir in the Libi block, Qinshui Basin, China. Advances in Civil Engineering, 2020. https://doi.org/10.1155/2020/6663496

Jaysaval P., Hammond G. E. and Johnson T. C. 2022. Massively Parallel Modeling and Inversion of Electrical Resistivity Tomography data using PFLOTRAN. March. https://gmd.copernicus.org/preprints/gmd-2022-66/

Krishnamurthy N. S., Rao, V. A., Kumar D., Singh K. K. K. and Ahmed S. 2009. Electrical Resistivity Imaging technique to delineate coal seam barrier thickness and demarcate water-filled voids. Journal of the Geological Society of India 2009 73: 5, 73(5): 639-650. https://doi.org/10.1007/S12594-009-0049-1

Little K. L., Hester E. T., Burbey T. J., Widdowson M. A., and Zipper C. E. 2018. Using Electrical Resistivity Imaging to Relate Surface Coal Mining Valley Fill Characteristics to Effluent Stream Quality Kathryn L. Little.

Loke M. H. 2015. 2-D and 3-D Electrical Imaging Surveys. Tutorial, May, 51-52.

Loke M. H., Alfouzan F. A. and Nawawi M. N. M. 2007. Optimisation of electrode arrays used in 2D resistivity imaging surveys. ASEG Extended Abstracts. 2007(1): 1-4. https://doi.org/10.1071/aseg2007ab002

Saad R., Nawawi M. N. M. and Mohamad E. T. 2012. Groundwater detection in alluvium using 2-D electrical resistivity tomography (ERT). Electronic Journal of Geotechnical Engineering. 17D (January): 369-376.

Sharma S. and Verma G. K. 2015. Inversion of Electrical Resistivity Data : A Review. World Academy of Science, Engineering, and Technology, International Journal of Environmental, Chemical, Ecological, Geological and Geophysical Engineering. 9(4): 392-398.

Taiwo A. 2017. Electrical Resistivity Imaging of a Coal Deposit at Tai Area of Gombe State, Electrical Resistivity Imaging of a Coal Deposit at Tai Area of Gombe State, North Eastern Nigeria. February 2016, 55-65.

Vu M., Xayavong V., Nguyen D., Vu T., Do C., Pham L. and Eldosouky A. 2021. Application of the Electrical

Resistivity Tomography and Seismic Refraction Methods for Groundwater Investigation in Savannakhet Province, Laos. Frontiers in Scientific Research and Technology, 0(0): 0-0. https://doi.org/10.21608/fsrt.2021.105000.1052

Zhou B. 2018. Electrical Resistivity Tomography: A Subsurface-Imaging Technique. Applied Geophysics with Case Studies on Environmental, Exploration, and Engineering Geophysics. https://doi.org/10.5772/INTECHOPEN.81511

Zubair M., Devi A., Israil M., Yogeshwar P. and Tezkan B. 2020. Application of Electrical Resistivity Tomography for Investigation of Shallow Subsurface HFT Zone in and around Mohand, Uttarakhand, India Geology and Geohydrology of the Study Area. E Journal of Geohydrogeology. 1(2): 47-55.